Silicon nanowire/polycaprolactone composites and their impact on stromal cell function

Ke Jiang and Jeffery L. Coffer[a)]
Department of Chemistry, Texas Christian University, Fort Worth, Texas 76129

Giridhar R. Akkaraju
Department of Biology, Texas Christian University, Fort Worth, Texas 76129

(Received 21 May 2012; accepted 20 July 2012)

In this study, silicon nanowire (SiNW)/polycaprolactone composites with different surface topographies were fabricated by straightforward embedding or printing methods and their cytocompatibility was evaluated with a bone-relevant cell line derived from mouse stroma. The incorporation of biocompatible polymers with semiconducting SiNWs can ideally provide an enhanced environment to support proliferation and differentiation functions of bone cells. Cell/composite interactions were assessed with suitable assays including viability and alkaline phosphatase activity, while scanning electron microscopy characterization was used to study the morphology of cells grown on composites. Such results suggest that for nanowires in a vertical array, the presence of the polymer improves cellular attachment and overall viability relative to the nanowire-only system.

I. INTRODUCTION

In the nanoscale regime, cell properties—viability, proliferation, differentiation—have been sensitive to surface topography of the biomaterial scaffold, as exemplified in the case of nanoposts,[1] nanotubes,[2] and nanoislands.[3] For the particular case of bone-related functions, it is widely accepted that an ideal orthopedic biomaterial must possess suitable surface features to allow the initial attachment and osteogenic differentiation of osteoprogenitor cells in vitro and in vivo.[4] Surface composition and associated energetics are also critical to ultimate tissue engineering functions.[5,6]

Silicon nanowires (SiNWs) are an intriguing candidate as a component in such structures, given their properties emerging from fundamental studies relevant to biosensors,[7,8] photonics,[9] and field-effect transistors.[10] More recently, considerable experiments have been undertaken to evaluate the role of SiNWs in affecting cellular functions or delivering biomolecules into cells,[11–15] including the role of surface chemistry.[16] Early work from our group suggested that SiNWs are cytocompatible (to fibroblasts),[17] readily functionalized to accommodate acellular calcification (through a calcium ion seed layer), with more recent studies demonstrating that sensitive changes in surface chemistry strongly influence the extent of proliferation of bone precursor cells.[18] Taking into account the fact that silicon has a major contributor to bone growth and early stages of mineralization,[19,20] we hypothesized that the integration of SiNWs in the development of novel composite biomaterials could provide a suitable environment to support bone cell functions and bone growth, thereby being potentially useful in bone tissue engineering applications.

Generally, a desirable tissue engineering scaffold should be adaptable to irregular wound sites.[21] Given the fact that SiNWs are usually grown on rigid and bioinert substrates (such as silicon wafers), the fabrication of SiNW devices on flexible and bioactive substrates is necessary for the manipulation of nanowire devices in a physiological environment. Recently, several approaches emerged to fabricate nanowire devices on flexible substrates. One strategy is referred to as the wet transfer method, in which single-crystalline nanowires were prepared and cast from solution onto plastic materials.[22] This method, however, is primarily used to fabricate two-dimensional devices for high-performance electronics such as SiNW-based transistors.[23] The other approach is referred to as the dry transfer method involving the relocation of SiNWs from original substrates to flexible substrates using poly(dimethylsiloxane) stamps or soluble glues.[24] Dry transfer has been used to prepare a variety of semiconductor nanowire devices onto plastics,[25,26] although these techniques generally involve complicated fabrication processes and their evaluation in a biological environment have not been reported.

In this approach, we begin with a baseline study to establish (i) the cytocompatibility of such composites, (ii) the role of nanowire orientation on the in vitro properties of these materials, and (iii) the ability of the

[a)]Address all correspondence to this author.
e-mail: j.coffer@tcu.edu
DOI: 10.1557/jmr.2012.265

 © Materials Research Society 2012

https://doi.org/10.1557/jmr.2012.265 Published online by Cambridge University Press

as-formed nanowire composites to impact cellular differentiation. For this purpose, SiNW/polycaprolactone (PCL) composites with different topographies were fabricated using two techniques. The first method, referred to as an embedding method, produces scaffolds with a horizontal network of nanowires embedded in a polymeric matrix. The second method, referred to as a printing method, generates a vertical nanowire array inserted in polymer substrates. PCL is selected as a substrate due to its slow degradation rate that is likely required for bone regeneration.[27] Such a composite material, therefore, is a promising candidate for implantable devices if a long-term therapeutic presence is desired.

In terms of experiments performed, the acellular calcification of calcium-seeded composites was investigated by immersion in simulated body fluid (SBF) at physiological temperature. To test the biocompatibility of these fabricated composite materials in vitro, mouse stromal cells (MSCs) were used to investigate the ability of different types of SiNW/PCL composites to support proliferation and differentiation of bone precursor cells. MSCs are derived from bone marrow and capable of differentiation into osteoblasts, chondrocytes, and adipocytes under the appropriate stimulus and environment.[28] Furthermore, realizing that cell attachment and spreading on a biomaterial are essential for regulating cell functions, scanning electron microscopy (SEM) imaging was used to evaluate the morphology of MSCs attached to SiNW/PCL composites.

II. EXPERIMENTAL

A. Synthesis of SiNWs

SiNWs were prepared by either a vapor–liquid–solid (VLS) method,[17] using gold as the catalyst and dilute silane (SiH_4) as silicon source, or an oxide-assisted VLS route,[29] using silicon monoxide as the precursor. Briefly, a Si wafer was cut into 7 × 10 mm pieces and coated with a 20-nm-thick layer of Au by radio frequency sputtering. In the VLS growth method, Au-coated substrates were heated to 600 °C and kept at this temperature for 1 h under helium (as carrier gas) at a flow rate of 300 standard cubic centimeters per minute (sccm). Diluted SiH_4 (0.5% in He, Voltaix, LLC, Branchburg, NJ) was then introduced into the reactor at a flow rate of 40 sccm for 20 min. In the oxide-assisted VLS growth method, 150 mg of SiO (Alfa Aesar, Ward Hill, MA) powder was loaded into an alumina boat located in the middle region of a tube furnace, with the Au-coated substrate located downstream at the edge of the tube furnace. A constant He flow of 40 sccm was introduced as an inert transport gas. The SiO was then heated to 1125 °C and kept at this temperature for 5 h, while the temperature of the growth region for the SiNWs is measured to be ~900 °C.

B. Fabrication of SiNW/PCL composites

Figure 1 shows a schematic illustration of the basic steps associated with the embedding and printing fabrication methods.

C. Printing method

SiNWs synthesized by the VLS method were used to fabricate composites by the printing method. A PCL (60 kDa, Aldrich, St. Louis, MO) platelet with a thickness of 0.2 mm was heated in the oven at 110 °C until the PCL platelet became transparent. Meanwhile, SiNWs (on a Si substrate) were heated at 110 °C for 30 min. Both PCL and SiNWs were then allowed to cool down in air simultaneously until the transparent PCL platelet just started to become opaque. The PCL film was then placed on top of the SiNWs and peeled off from it after cooling.

D. Embedding method

SiNWs used in this method were synthesized by the oxide-assisted VLS route. One piece of a PCL film (1 × 1 cm) with thickness of 0.07 mm was placed on top of a SiNW sample and 0.5 mL of chloroform was dropped on top of a PCL film at a rate of 1 drop per 2 s. After the complete evaporation of chloroform, another piece of PCL film was added and etched with the same amount of chloroform again at the same dropping rate. In total, up to four pieces of PCL film (per SiNW/Si substrate sample) were incorporated with SiNWs by this method.

E. Acellular calcification assay of SiNW/PCL composites

Calcification assays of SiNW/PCL composites were carried out by an electrochemical method reported previously.[17,18] Briefly, SiNWs were seeded with Ca^{2+} by a cathodic bias process in SBF as the electrolyte. SBF is composed of ions commonly present in plasma, without the serum proteins. The SBF solution contained the following salt concentrations: $CaCl_2$, 2.5 mM; Na_2SO_4, 0.5 mM; NaCl, 135.8 mM; KCl, 4.0 mM; $MgCl_2$, 1.5 mM; $NaHCO_3$, 4.2 mM; K_2HPO_4, 1.0 mM. The pH value of SBF was adjusted to be 7.25–7.35 by Trizma base and 0.7 M HCl solution. The applied current density was 5 mA/cm^2 and the bias duration was 120 min. After bias, SiNWs were incorporated with PCL by either the printing method or the embedding method. The SiNW/PCL composites were then soaked in SBF at 37 °C for 6 wk. In control experiments, as-prepared SiNWs without being seeded with Ca^{2+} ions were incorporated with PCL by embedding/printing methods and soaked in SBF at 37 °C afterward.

F. Attachment of MSCs on SiNW/PCL composites

Prior to cell attachment experiments, SiNW/PCL composites were soaked in 70% ethanol for 24 h,

https://doi.org/10.1557/jmr.2012.265 Published online by Cambridge University Press

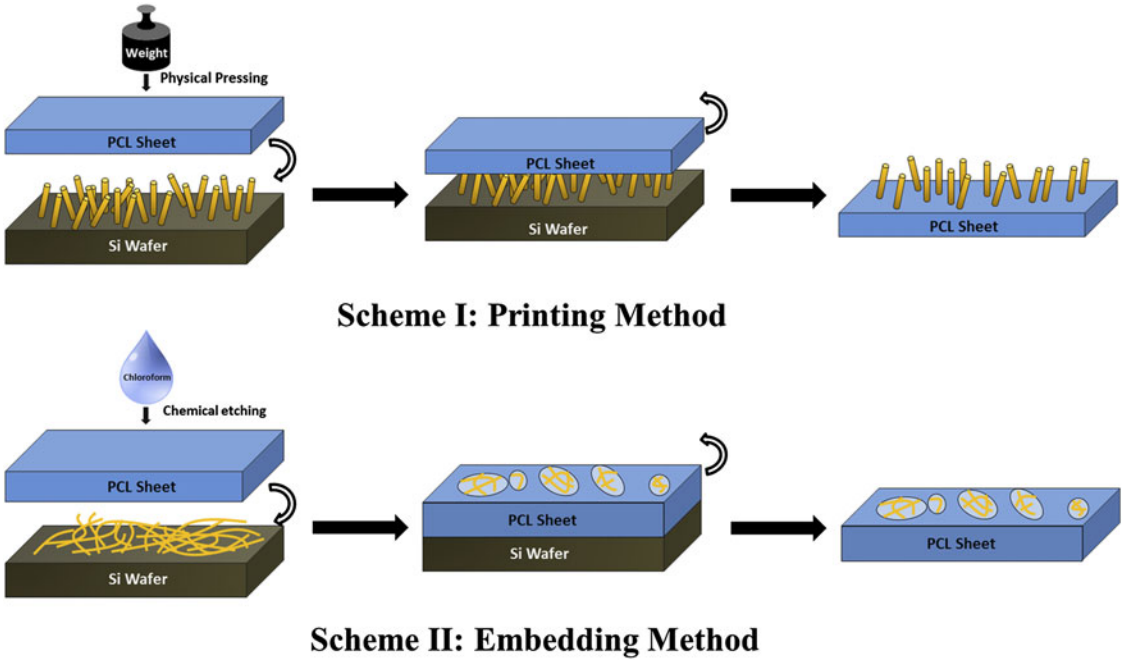


FIG. 1. Schematic illustration of (a) Printing and (b) Embedding methods for SiNW/PCL composite structures.

followed by immersion in sterilized deionized water for 5 min. After drying, samples were further sterilized by exposure to ultraviolet light for 2 h. MSCs (D1-ORL-UVA, ATCC number CRL-12424) were seeded at a density of 35,000 cells or 10,000 cells onto each composite prepared by the embedding method or the printing method, respectively, in 12-well cell culture plates. The cells were fed every 3 days using complete growth medium [Eagle's minimal essential medium (DMEM), 10% Fetal Bovine Serum, 1% Penicillin/Streptomycin]. Cell attachment was characterized by SEM imaging (JEOL JSM-6100, Tokyo, Japan) after being cultured for 7 days. SiNWs grown on Si wafers by either the VLS method or the oxide-assisted VLS route were used as controls.

Before SEM characterization, samples were washed by phosphate buffered saline (PBS) to remove the dead cells before fixation. The fixative was prepared by mixing 30 mL of 8% glutaraldehyde, 30 mL of 6% paraformaldehyde, and 30 mL of phosphate buffered solution, which was prepared by mixing 19 mL of 0.2 M NaH_2PO_4 solution and 81 mL of 0.2 M Na_2HPO_4 solution and diluting to 200 mL with DI water. Composites were then soaked in the fixative for 2 h at room temperature and dehydrated by passing through a series of ethanol solutions with increasing concentrations (30%, 50%, 70%, 85%, 95%, and 100%) and then two more portions of 100% alcohol, followed by soaking in pure hexamethyldisilazane overnight. After air drying, the dehydrated samples were sputter-coated with a 20-nm-thick gold layer before SEM characterization.

G. Viability assays

The viability of MSCs was studied by a 3-(4,5-dimethylthiazol-2-yl)-2,5-diphenyl tetrazolium bromide (MTT, Sigma, St. Louis, MO) assay in the presence of SiNW/PCL composites. SiNWs were used as controls. After sterilization of composites, 10,000 MSCs were cultured on each sample in 12-well cell culture plates and 1 mL of complete growth medium was added into each well. At designated time points (3, 5, and 7 days), growth medium was aspirated from each well, followed by rinsing with 1 mL sterilized PBS. 0.5 mL of MTT working solution (1 mg/mL) in serum-free medium (DMEM) was added to each cell culture well. The cell culture plate was incubated at 37 °C, 5% CO_2 for 4 h. After removal of supernatant, 1 mL of dimethyl sulfoxide (DMSO) was added into each well and allowed to dissolve the precipitate for 5 min. After a 10-fold dilution with DI water, the optical density of each solution was measured by a spectrophotometer (Beckman, DU-64, Brea, CA) at a wave length of 540 nm. Pure DMSO was used as the blank. The experiments were performed in triplicate.

H. Alkaline phosphatase assays

The differentiation of MSCs was measured by quantifying the alkaline phosphatase (ALP) activity of cells cultured on SiNW/PCL composites. SiNWs were used as controls. After sterilization of the selected materials, MSCs were plated onto the composites in a 12-well cell culture plate at a density of 10,000 cells/well. The MSCs cultured in all wells were fed with complete growth

https://doi.org/10.1557/jmr.2012.265 Published online by Cambridge University Press

medium on day 0. Half of the wells for each type of samples were then switched to differentiation medium on day 1, and the cells in the other half of the wells were continued to be fed by complete growth medium. The differentiation medium was DMEM supplemented with 10 mM β-glycerol phosphate, 0.05 mM ascorbic acid 2-phosphate, 100 nM dexamethasone, 10% fetal bovine serum (FBS), and 1% penicillin/streptomycin. At the designated time point, the medium was aspirated and 1 mL PBS was added into each well to wash the cells. A volume of 500 μL lysis buffer (5 mM $MgCl_2$, 1% Triton in DI water) was added to each cell culture well before being placed onto a shaker on ice for 10 min. p-nitrophenyl phosphate (pNPP) solution (1 mg/mL) was prepared by dissolving one pNPP tablet and one Tris buffer tablet from a pNPP kit (Sigma-Aldrich, St. Louis, MO) into 20 mL of DI water. 100 μL of such solution was added to 80 μL lysate and stirred via vortex mixing. The solution was then incubated in a water bath at 37 °C for 2 h. 100 μL of 0.2 M NaOH solution was added into the incubated solution to stop the reaction. The solution was mixed again with vortex mixing followed by measuring the absorbance at 405 nm spectrophotometrically. DI water was used as a blank. The experiments were performed in triplicate.

III. RESULTS AND DISCUSSION

A. Morphology of SiNWs and SiNW/PCL composites

Under the conditions utilized, SiNWs prepared by a VLS method with silane as the Si source have an average diameter of 166 ± 48 nm [Fig. S1(a)], as evaluated by SEM imaging [Fig. 2(a)]. This type of SiNWs is suitable for making composites by the printing method since most nanowires have one end exposed and can easily be inserted into another soft substrate through that exposed end. On the other hand, the oxide-assisted VLS route generates SiNWs of a dense, curved, entangled morphology [Fig. 2(b)] with an average diameter of 85 ± 21 nm [Fig. S1(b)]. It is challenging for this latter type of nanowire to be inserted vertically into a polymer substrate and thus is better suited for making horizontal NW arrays by the embedding method. The morphology of SiNW/PCL composites fabricated by the printing method is shown in Fig. 2(c). Most SiNWs (with lengths up to tens of micrometers) are vertically aligned on the PCL platelet due to the nature of this printing transfer method. In contrast, composites fabricated by the embedding method consist of a web-like morphology of PCL and horizontally aligned SiNW bundles at the bottom of the open areas of the film [Fig. 2(d)]. A layer of SiNW/PCL composites can be peeled off from the underlying silicon wafer to form a freestanding composite material (see Supplementary Material).

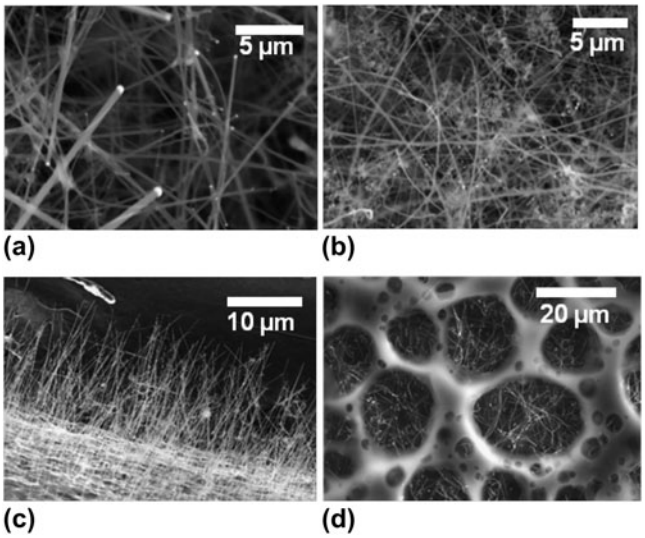


FIG. 2. (a) SiNWs synthesized by the VLS method; (b) SiNWs synthesized by the oxide-assisted VLS method; (c) SiNW/PCL composites fabricated by the printing method; and (d) SiNW/PCL composites fabricated by the embedding method.

B. Acellular calcification of SiNW/PCL composites

As shown in Fig. 3, calcium-seeded SiNWs induced significant calcification on both types of SiNW/PCL composites (printing and embedding methods) after soaking in SBF at 37 °C for 6 wk. The surfaces of SiNW/PCL composites are fully covered by a thick layer of calcium phosphate, which is confirmed by the energy-dispersive spectroscopy analysis. In control experiments, non-Ca^{2+}-seeded SiNWs did not induce the growth of detectable amounts of calcium phosphate on SiNW/PCL composites (data not shown). Such observations are consistent with earlier measurements on the individual components, the as-prepared SiNWs as well as the PCL substrate. As in the case of the SiNWs, it is necessary to form initial calcium phosphate nucleation sites on a given nanowire surface via a brief cathodic bias step in the presence of a dilute aqueous solution of Ca^{2+} to induce the uniform formation of the target calcified phase.[17] Nevertheless, as expected, extensive calcification takes place throughout the exposed surface of the composite.

C. Attachment of MSC on SiNW/PCL composites

Figure 4 shows the morphology of MSCs after being cultured for 7 days on selected materials. When cultured on SiNWs alone synthesized by either VLS or oxide-assisted VLS methods, MSCs showed a rounded shape and restricted spreading [Figs. 4(a) and 4(b)]. In contrast, MSCs on SiNW/PCL composites fabricated by the embedding method showed elongated shapes with multiple filopodia stretching out and attaching to the composite underneath [Fig. 4(c)]. For MSCs grown on SiNW/PCL composites fabricated by the printing method [Fig. 4(d)], the penetration of SiNWs through cells is clearly visible.

https://doi.org/10.1557/jmr.2012.265 Published online by Cambridge University Press

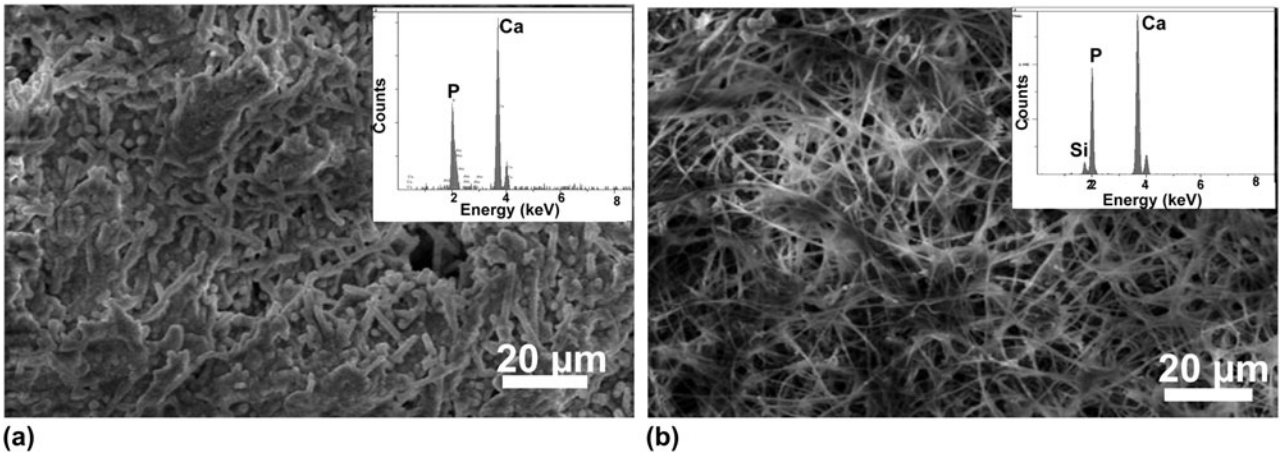


FIG. 3. (a) Calcification of SiNW/PCL composite fabricated by the printing method; (b) calcification of SiNW/PCL composite fabricated by the embedding method. SiNWs were coated with Ca^{2+} seeds by a cathodic bias process for 120 min at a current density of 5 mA/cm^2. Composites with Ca^{2+}-seeded SiNWs were soaked in SBF at 37 °C for 6 wk under zero bias. Insets show the energy dispersive x-ray spectroscopy (EDX) spectra, confirming the presence of calcium and phosphorous.

The shape of the cell was distorted and apparently affected by the presence of the surrounding SiNWs. It should also be pointed out that in the case of composites prepared by the embedding method, long-range alignment of cells is observed upon extended periods of exposure (3 wk) (see Supplementary Material).

Attachment of cells on these materials likely takes place through formation of specialized supramolecular protein complexes called focal adhesions.[30] Such adhesions not only serve as the mechanical linkages to the surface of biomaterial but also as a biochemical signaling hub to concentrate and direct numerous signaling proteins at sites of integrin binding and clustering. Variations in nanoscale topography of the substrate can modulate adhesion assembly,[31–33] resulting in the regulation of cell behavior by altering signaling pathways.[30] In our experiments, SiNWs with no PCL content greatly restricted the cell spreading, due presumably to a lack of focal adhesion and filopodia formation, thereby limiting MSC attachment and migration. It would appear that the polymer material fused with SiNWs provides a necessary basement for cells to attach and migrate.

While embedded SiNWs in a PCL matrix can (not surprisingly) successfully support cell adhesion and spreading, vertically aligned SiNWs on flat PCL substrates can also support cell growth without inducing significant cell death by penetration. These results are consistent with those reported previously by Yang et al.,[34] who showed that the engulfment of vertically oriented SiNWs (on Si surfaces) by cells did not induce cell death; rather DNA immobilized on SiNWs could be delivered into cells with the nanowire acting as a vector. Other studies have shown that vertical SiNWs can be used to guide neuronal progenitor growth, knock down transcript levels, inhibit apoptosis, and introduce targeted proteins to specific organelles by impaling and delivering biomolecules into living cells.[35]

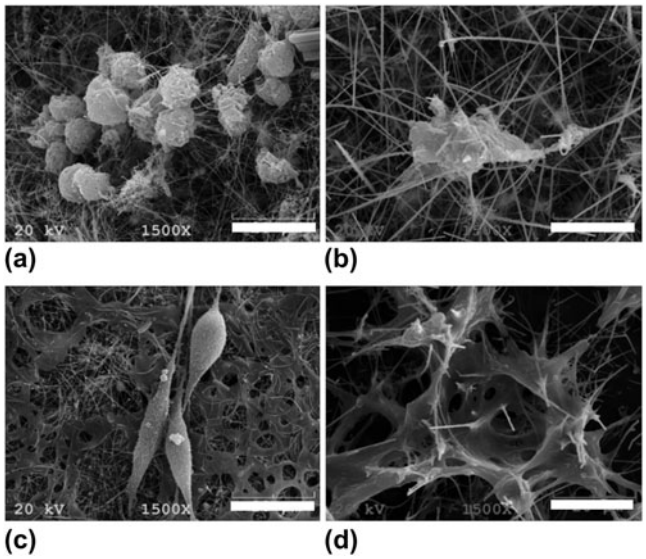


FIG. 4. SEM images of MSCs cultured on (a) SiNWs synthesized by the oxide-assisted VLS method; (b) SiNWs synthesized by the VLS method; (c) SiNW/PCL composite fabricated by the embedding method; (d) SiNW/PCL composite fabricated by the printing method. Scale bar = 20 μm.

D. Viability of MSCs on SiNW/PCL composites

The viability of MSCs on SiNW/PCL composites was investigated by the MTT assay, a simple and accurate colorimetric assay for measuring cell viability in vitro.[36] As shown in Fig. 5, cells grown on SiNW/PCL composites exhibited increased viabilities as the culturing time increases. The viability of MSCs on SiNW/PCL composites is higher than those grown on SiNW surfaces, with

https://doi.org/10.1557/jmr.2012.265 Published online by Cambridge University Press

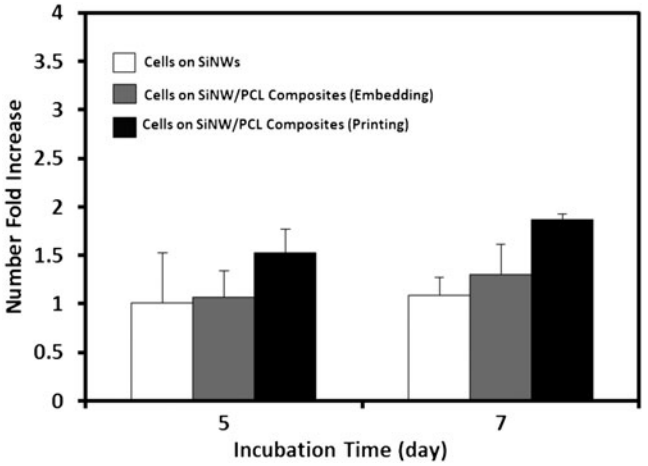


FIG. 5. Viability of MSCs by the MTT assay. The cells are affected by surface features of different substrates. SiNWs as a control substrate were synthesized by the VLS method. Each value represents the average ± SD ($n = 3$).

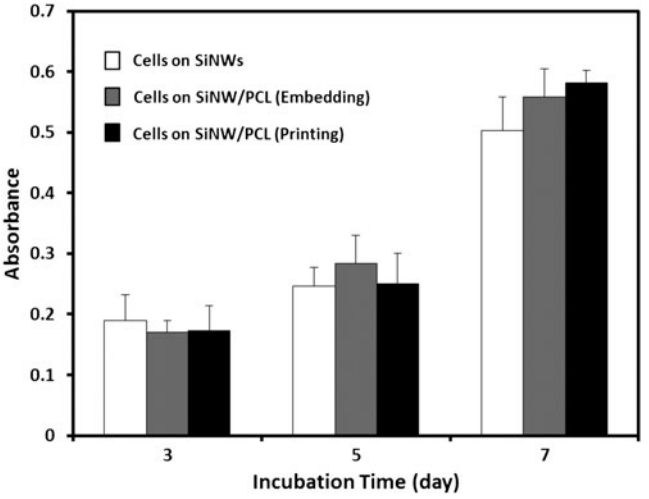


FIG. 6. ALP activity of MSCs cultured on different substrates. Absorbance is an indicator of cellular differentiation. SiNWs as a control substrate were synthesized by the VLS method. Each value represents the average ± SD ($n = 3$).

composites fabricated by the printing method exhibiting a higher viability than those grown on composites fabricated by the embedding method.

The observed lowest viability of cells cultured on SiNW surfaces is consistent with cell attachment experiments in which stromal cells generally showed rounded shapes as a sign of their unhealthy status. It is unclear that why MSCs grown on the vertical SiNWs exhibit higher viability than those grown on horizontal SiNW/PCL surfaces. As reported previously, the transcript levels of five common housekeeping genes of HeLa S3 cells and human fibroblasts cultured on vertical SiNWs are similar to those in cells cultured on multiwell plates, indicating that perturbations of cell growth induced by vertical SiNWs might be negligible.[35] Although the observed deviations might be attributed to a cell-dependent manner or high sensitivity of cells to changes of external surface features, details of cell physiology response to nanowire penetration are a topic of future investigation.

E. Differentiation of MSC on SiNW/PCL composites

Osteogenic differentiation of MSCs cultured on SiNW/PCL composites was assessed by an analysis of ALP activity.[37] As shown in Fig. 6, the ALP activity of MSCs cultured on SiNW/PCL composites increased steadily with increasing culturing time, and there is a small but statistically insignificant greater level of ALP expression for stromal cells interacting with SiNW/PCL composites prepared by the printing method. Based on chemical similarities between platforms, similar differentiation behavior is anticipated.

In the future, additional refinement of differentiation behavior in these nanowire composites can possibly be achieved by additional chemical modifications such as coupling of synthetic biomimetic peptides[38] or bone morphogenetic protein[39–41] onto composite surfaces.

IV. CONCLUSIONS

The results described above clearly demonstrate straightforward routes to the fabrication of SiNW/PCL composites with either horizontally or vertically aligned SiNW arrays, which provides opportunities for the facile generation of composite nanoscale biomaterials for possible tissue engineering applications. Acellular calcification, along with stromal cell attachment and proliferation, is readily observed in such composites. Future opportunities will likely entail more detailed studies on the impact of chemical modification on the cell specific in vitro response, as well as fabrication of three-dimensional composite scaffolds with appropriate porosities and mechanical characteristics.

ACKNOWLEDGMENT

Financial support by the Robert A. Welch Foundation (Grant P-1212) is gratefully acknowledged.

REFERENCES

1. C.H. Choi, S.H. Hagvall, B.M. Wu, J.C.Y. Dunn, R.E. Beygui, and C.J. Kim: Cell interaction with three-dimensional sharp-tip nanotopography. *Biomaterials* **28**, 1672–1679 (2007).
2. S. Garibaldi, C. Brunelli, V. Bavastrello, G. Ghigliotti, and C. Nicolini: Carbon nanotube biocompatibility with cardiac muscle cells. *Nanotechnology* **17**, 391–397 (2006).

https://doi.org/10.1557/jmr.2012.265 Published online by Cambridge University Press

3. M.J. Dably, M.O. Riehle, H. Johnstone, S. Affrossman, and A.S.G. Curtis: In vitro reaction of endothelial cells to polymer demixed nanotopography. *Biomaterials* **23**, 2945–2954 (2002).
4. S.L. Ishaug, G.M. Crane, M.J. Miller, A.W. Yasko, M.J. Yaszemski, and A.G. Mikos: Bone formation by three-dimensional stromal osteoblast culture in biodegradable polymer scaffolds. *J. Biomed. Mater. Res.* **36**, 17–28 (1997).
5. Z. Shwartz and B.D. Boyan: Underlying mechanisms at the bone–biomaterial interface. *J. Cell. Biochem.* **56**, 340–347 (1994).
6. J. Lee, B.S. Kang, B. Hicks, T.F. Chancellor, Jr., B.H. Chu, H.T. Wang, B.G. Keselowsky, F. Ren, and T.P. Lele: The control of cell adhesion and viability by zinc oxide nanorods. *Biomaterials* **29**, 3743–3749 (2008).
7. Y. Cui, Q. Wei, H. Park, and C.M. Lieber: Nanowire nanosensors for highly sensitive and selective detection of biological and chemical species. *Science* **293**, 1289–1292 (2001).
8. M.W. Shao, H. Yao, M.L. Zhang, N.B. Wong, Y.Y. Shan, and S.T. Lee: Fabrication and application of long strands of silicon nanowires as sensors for bovine serum albumin detection. *Appl. Phys. Lett.* **87**, 183106 (2005).
9. M.S. Gudiksen, L. Lauhon, L. Wang, D. Smith, and C.M. Lieber: Growth of nanowire superlattice structures for nanoscale photonics and electronics. *Nature* **415**, 617–620 (2002).
10. Y. Cui and C.M. Lieber: Functional nanoscale electronic devices assembled using silicon nanowire building blocks. *Science* **291**, 851–853 (2001).
11. K.C. Popat, R.H. Daniels, R.S. Dubrow, V. Hardev, and T.A. Desai: Nanostructured surfaces for bone biotemplating applications. *J. Orthop. Res.* **24**, 619–627 (2006).
12. H. Kwon, M.F. Beaux, II, C. Ebert, L. Wang, B.E. Lassiter, Y.H. Park, D.N. Mcllroy, C.J. Hovde, and G.A. Bohach: Nanowire-based delivery Escherichia coli O157 Shiga toxin 1 A subunit into human bovine cells. *Nano Lett.* **7**, 2718–2723 (2007).
13. K.S. Brammer, C. Choi, S. Oh, C.J. Cobb, L.S. Connelly, M.S. Loya, D. Kong, and S. Jin: Antibiofouling, sustained antibiotic release by Si nanowire templates. *Nano Lett.* **9**, 3570–3574 (2009).
14. S. Qi, C. Yi, W. Chen, C.C. Fong, S.T. Lee, and M. Yang: Effects of silicon nanowires on HepG2 cell adhesion and spreading. *ChemBioChem* **8**, 1115–1118 (2007).
15. S. Qi, C. Yi, S. Ji, C.C. Fong, and M. Yang: Cell adhesion and spreading behavior on vertically aligned silicon nanowire arrays. *ACS Appl. Mater. Interfaces* **1**, 30–34 (2009).
16. G. Piret, E. Galopin, Y. Coffinier, R. Boukherroub, D. Legrand, and C. Slomianny: Culture of Mammalian Cells on Patterned Superhydrophilic/Superhydrophobic Silicon Nanowire Arrays. *Soft Matter* **7**, 8642–8649 (2011).
17. D.K. Nagesha, M.A. Whitehead, and J.L. Coffer: Biorelevant calcification and non-cytotoxic behavior in silicon nanowires. *Adv. Mater.* **17**, 921–924 (2005).
18. K. Jiang, D. Fan, Y. Belabassi, G.R. Akkaraju, J-L. Montchamp, and J.L. Coffer: Medicinal surface modification of silicon nanowires: Impact on calcification and stromal cell proliferation. *ACS Appl. Mater. Interfaces* **1**, 266–269 (2009).
19. E.M. Carlisle: In vivo requirement for silicon in articular cartilage and connective tissue formation in the chick. *J. Nutr.* **106**, 478–484 (1976).
20. E.M. Carlisle: Biochemical and morphological changes associated with long bone abnormalities in silicon deficiency. *J. Nutr.* **110**, 1046–1056 (1980).
21. K.J.L. Burg, S. Porter, and J.F. Kellam: Biomaterial developments for bone tissue engineering. *Biomaterials* **21**, 2347–2359 (2000).
22. E.J. Snyder, J. Chideme, and G.S.W. Craig: Fluidic self-assembly of semiconductor devices: A promising new method of mass-producing flexible circuitry. *Jpn. J. Appl. Phys.* **41**, 4366–4369 (2002).
23. X. Duan, C. Niu, V. Sahi, J. Chen, J.W. Parce, S. Empedocles, and J.L. Goldman: High-performance thin-film transistors using semiconductor nanowires and nanoribons. *Nature* **425**, 274–278 (2003).
24. J.H. Ahn, H.S. Kim, K.J. Lee, S. Jeon, S.J. Kang, Y. Sun, R.G. Nuzzo, and J.A. Rogers: Heterogeneous three-dimensional electronics by use of printed semiconductor nanomaterials. *Science* **314**, 1754–1757 (2006).
25. Y. Sun, S. Kim, I. Adesida, and J.A. Rogers: Bendable GaAs metal-semiconductor field-effect transistors formed with printed GaAs wire arrays on plastic substrates. *Appl. Phys. Lett.* **87**, 083501 (2005).
26. K.J. Lee, J. Lee, H. Hwang, Z.J. Reitmeier, R.F. Davis, J.A. Rogers, and R.G. Nuzzo: A printable form of single-crystalline gallium nitride for flexible optoelectronic systems. *Small* **1**, 1164–1168 (2005).
27. C.X.F. Lam, D.W. Hutmacher, J.T. Schantz, M.A. Woodruff, and S.H. Teoh: Evaluation of polycaprolactone scaffold degradation for 6 months in vitro and in vivo. *J. Biomed. Mater. Res.* **90A**, 906–919 (2009).
28. R.S. Tuan, G. Boland, and R. Tuli: Adult mesenchymal stem cells and cell-based tissue engineering. *Arthritis Res. Ther.* **5**, 32–45 (2003).
29. F.M. Kolb, H. Hofmeister, R. Scholz, M. Zacharias, U. Gosele, D.D. Ma, and S.T. Lee: Analysis of silicon nanowires grown by combining SiO evaporation with the VLS mechanism. *J. Electrochem. Soc.* **151**, G472–G475 (2004).
30. A. Bershadsky, M. Kozlov, and B. Geiger: Adhesion-mediated mechanosensitivity: A time to experiment, and a time to theorize. *Curr. Opin. Cell Biol.* **8**, 472–481 (2006).
31. J.P. Spatz and B. Geiger: Molecular engineering of cellular environments: Cell adhesion to nano-digital surfaces. *Methods Cell Biol.* **83**, 89–111 (2007).
32. M. Arnold, E.A. Cavalcanti-Adam, R. Glass, J. Blummel, W. Eck, M. Kantlehner, H.J. Kessler, and P. Spatz: Activation of integrin function by nanopatterned adhesive interfaces. *ChemPhysChem* **5**, 383–388 (2004).
33. E.A. Cavalcanti-Adam, T. Volberg, A. Micoulet, H. Kessler, B. Geiger, and J.P. Spatz: Cell spreading and focal adhesion dynamics are regulated by spacing of integrin ligands. *Biophys. J.* **92**, 2964–2974 (2007).
34. K. Woong, J.K. Ng, M.E. Kunitake, B.R. Conklin, and P.D. Yang: Interfacing silicon nanowires with mammalian cells. *J. Am. Chem. Soc.* **129**, 7228–7229 (2007).
35. A.K. Shalek, J.T. Robinson, E.S. Karp, J.S. Lee, D.R. Ahn, M.H. Yoon, A. Sutton, M. Jorgolli, R.S. Gertner, T.S. Gujral, G. MacBeath, E.G. Yang, and H. Park: Vertical silicon nanowires as a universal platform for delivering biomolecules into living cells. *Proc. Natl. Acad. Sci. U.S.A.* **107**, 1870–1875 (2010).
36. T. Mosmann: Rapid colorimetric assay for cellular growth and survival: Application to proliferation and cytotoxicity assays. *J. Immunol. Meth.* **65**, 55–63 (1983).
37. O.A. Bessey, O.H. Lowry, and M.J. Brock: A method for the rapid determination of alkaline phosphatase with five cubic millimeters of serum. *J. Biol. Chem.* **164**, 321–329 (1946).
38. H. Egusa, Y. Kaneda, Y. Akashi, Y. Hamada, T. Matsumoto, M. Saeki, D.K. Thakor, Y. Tabata, N. Matsuura, and H. Yatani: Enhanced bone regeneration via multimodal actions of synthetic peptide SVVYGLR on osteoprogenitors and osteoclasts. *Biomaterials* **30**, 4676–4686 (2009).
39. U. Ripamonti and N. Duneas: Tissue morphogenesis and regeneration by bone morphogenetic proteins. *Plast. Reconstr. Surg.* **101**, 227–239 (1998).
40. M.P. Bostrom and N.P. Camacho: Potential role of bone morphogenetic proteins in fracture healing. *Clin. Orthop. Relat. Res.* **355**, S274–S282 (1998).

https://doi.org/10.1557/jmr.2012.265 Published online by Cambridge University Press

41. T.K. Sampath, J.C. Maliakal, P.V. Hauschka, W.K. Jones, H. Sasak, R.F. Tucker, K.H. White, J.E. Coughlin, M.M. Tucker, R.H.L. Pang, C. Corbett, E. Ozkaynak, H. Oppermann, and D.C. Rueger: Recombinant human osteogenic protein-1 (hOP-1) induces new bone formation in vivo with a specific activity comparable with natural bovine osteogenic protein and stimulates osteoblast proliferation and differentiation in vitro. *J. Biol. Chem.* **267**, 20352–20362 (1992).

Supplementary Material

Supplementary material can be viewed in this issue of the *Journal of Materials Research* by visiting http://journals.cambridge.org/jmr.

https://doi.org/10.1557/jmr.2012.265 Published online by Cambridge University Press